Monthly Notices
of the
ROYAL ASTRONOMICAL SOCIETY

Mon. Not. R. Astron. Soc. **426,** 2452–2462 (2012) doi:10.1111/j.1365-2966.2012.21784.x

A comprehensive comparison of cosmological models from the latest observational data

K. Shi,[1,2] Y. F. Huang[1,2]★ and T. Lu[3,4]

[1]*Department of Astronomy, Nanjing University, Nanjing 210093, China*
[2]*Key Laboratory of Modern Astronomy and Astrophysics (Nanjing University), Ministry of Education, Nanjing 210093, China*
[3]*Purple Mountain Observatory, Chinese Academy of Sciences, Nanjing 210008, China*
[4]*Joint Center for Particle, Nuclear Physics and Cosmology, Nanjing University – Purple Mountain Observatory, Nanjing 210093, China*

Accepted 2012 July 24. Received 2012 July 13; in original form 2012 April 5

ABSTRACT

We carry out a detailed investigation of some popular cosmological models in light of the latest observational data, including the Union2.1 supernovae compilation, the baryon acoustic oscillation measurements from the WiggleZ Dark Energy Survey and the cosmic microwave background information from the *Wilkinson Microwave Anisotropy Probe* seven-year observations, along with the observational Hubble parameter data. Based on the selection statistics of the models, such as the Akaike and the Bayesian information criteria, we compare different models to assess their worth. We do not assume a flat universe in the fitting. Our results show that the concordance Λ cold dark matter (CDM) model remains the best model to explain the data, while the Dvali–Gabadadze–Porrati model is clearly not favoured by the data. Among these models, the models whose parameters can reduce themselves to the ΛCDM model provide good fits to the data. These results indicate that for the current data, there is no obvious evidence to support the use of any more complex models over the simplest ΛCDM model.

Key words: cosmological parameters – cosmology: observations – cosmology: theory – dark energy.

1 INTRODUCTION

The present accelerating expansion of the Universe is a great challenge to our fundamental physics and cosmology. This fact was first discovered from Type Ia supernova (SNIa) surveys (Riess et al. 1998; Perlmutter et al. 1999). Later, it was confirmed by the precise measurement of cosmic microwave background (CMB) anisotropies (Spergel et al. 2003) as well as baryon acoustic oscillations (BAOs) in the luminous galaxy sample of the Sloan Digital Sky Survey (SDSS; Eisenstein et al. 2005). This cosmic acceleration has led us to believe that most energy in the Universe exists in the form of a new ingredient called dark energy, which has a negative pressure.

Various theoretical models of dark energy have been proposed, the simplest being the cosmological constant Λ with constant dark energy density and equation of state $w_{\rm DE} = p/\rho = -1$. This model, the popular Λ cold dark matter (CDM) model, has so far provided an excellent fit to a wide range of observational data. Despite its simplicity and success, the ΛCDM model has two problems. One is the so-called fine-tuning problem; that is, the observed value of Λ is extremely small compared with the expectations of particle physicists (Weinberg 1989). The other is the coincidence problem; that is, the present energy density of dark energy Ω_Λ and the present matter density $\Omega_{\rm m}$ are of the same order of magnitude, for no obvious physical reasons. Because of these difficulties with the cosmological constant, numerous alternative models, instead of the ΛCDM model, have been proposed to explain the acceleration (for recent reviews, see Copeland, Sami & Tsujikawa 2006; Frieman, Turner & Huterer 2008). Generally speaking, these models can be divided into two groups: in one group, the matter is modified (i.e. the right-hand side of the Einstein equation) and in the other group, the gravity is modified (i.e. the left-hand side of the Einstein equation).

Although most studies have shown that the ΛCDM model is in good agreement with observational data, dynamical dark energy cannot yet be excluded. In order to distinguish between different dark energy models from observations, the most commonly used method is to constrain the dark energy equation of state w. Recent studies have already given tight constraints on w. For example, the Supernova Legacy Survey three-year sample (SNLS3), combined with other probes, has given $w = -1.061 \pm 0.068$ (Sullivan et al. 2011). It should be noted that although these results are consistent with the ΛCDM model, we cannot yet determine whether the density of dark energy is actually constant, or whether it varies with time, as suggested by dynamical models.

When a new cosmological model is proposed, it is very important to place constraints on the model parameters. Usually, a maximum likelihood estimate is used to set constraints on the parameters of the

★E-mail: hyf@nju.edu.cn

model. If the expected distribution of the data is Gaussian (which is applicable for most problems in cosmology), we can use the familiar χ^2 test for parameter estimation (i.e. the smaller χ^2 is, the better the parameters fit the data).

However, because there are so many different dark energy models, a natural question arises. Which model is better or, in other words, which model is most favoured by the current observational data? This is the problem of model selection. We might naïvely apply the χ^2 test here, but this does not contain the information of the complexity (the number of parameters) of different models. That is, χ^2 statistics are good at finding the best-fitting parameters in a model but they are insufficient for deciding whether this model itself is the best model. In order to solve this problem, some model selection statistics have been proposed in the context of cosmology (Liddle 2004; Davis et al. 2007). The most commonly used is the information criteria (ICs) including the Akaike information criterion (AIC; Akaike 1974) and the Bayesian information criterion (BIC; Schwarz 1978). These criteria tend to favour models that give a good fit with fewer parameters, which embody the spirit of Occam's razor: 'entities must not be multiplied beyond necessity'.

In this paper, we investigate the parameter constraints on a number of cosmological models by performing a Markov chain Monte Carlo (MCMC) analysis using the latest observational data. Then, we apply the model selection statistics to compare different models, in order to assess which is preferred or disfavoured by the data. We have organized our paper as follows. In Section 2, we discuss the model comparison statistics used in this paper. In Section 3, we describe the observational data used in this paper and the method for their use. In Section 4, we give a detailed description of the different cosmological models to be tested and the constraining results from observations. In Section 5, we give a comparison of the different models by using model selection statistics. We present our discussion and conclusions in the last section.

2 MODEL SELECTION STATISTICS

As mentioned in Section 1, we mainly use the ICs, including the AIC and the BIC, to test different models. A detailed description of the AIC and the BIC has been given by Liddle (2004). The AIC is given by

$$\mathrm{AIC} = -2\ln\mathcal{L}_{\max} + 2k, \tag{1}$$

where $\mathcal{L}_{\max}$ is the maximum likelihood and k is the number of parameters. Note that for the Gaussian posterior distribution, $\chi^2_{\min} = -2\ln\mathcal{L}_{\max}$. The AIC was derived from information theoretical considerations.

The BIC is defined as

$$\mathrm{BIC} = -2\ln\mathcal{L}_{\max} + k\ln N, \tag{2}$$

where N is the number of data points used in the fit. The BIC is similar to the AIC, but it includes the number of data points in its form while the AIC does not. Note that for any likely data set, $\ln N > 2$, and thus the BIC imposes a stricter penalty against extra parameters than the AIC. However, the AIC remains useful because it gives an upper limit to the number of parameters that should be included. The BIC was derived as an approximation to the Bayesian evidence, but this approximation is quite crude.

The preferred model is the one that minimizes the AIC and the BIC. However, their absolute values are not of interest; only the relative value between different models makes sense.

For the AIC, Burnham & Anderson (2003) have featured the following 'strength of evidence' in the form of $\Delta\mathrm{AIC} = \mathrm{AIC}_i - \mathrm{AIC}_{\min}$:

ΔAIC, level of empirical support for model i;
0–2, substantial;
4–7, considerably less;
>10, essentially none.

For the BIC, Robert & Adrian (1995) have featured the following strength of evidence, where $\Delta\mathrm{BIC} = \mathrm{BIC}_i - \mathrm{BIC}_{\min}$:

ΔBIC, evidence against model i;
0–2, not worth more than a bare mention;
2–6, positive;
6–10, strong;
>10, very strong.

Thus, we can first obtain a model that minimizes the ICs, and then we can compare the rest of the models with it, using the above judgements as strength of evidence.

It should be noticed that the ICs alone can, at most, indicate that a more complex model is not necessary to explain the data, because a poor IC might rise from the fact that the data are too poor to constrain the extra parameters in the model, and this model might be preferred if improved data were available.

Furthermore, we must be aware of the limitation of using these simplified ICs, because they are based on the best-fitting χ^2. A more in-depth analysis of model selection should consider how much parameter space would give data with high probability, as well as the correlations between the parameters. The Bayesian evidence is an approach that takes this into account; it computes the average likelihood of a model over its prior parameter ranges. For further discussion, see, for example, Saini, Weller & Bridle (2004), Liddle (2007) and Trotta (2007). However, the Bayesian evidence requires that we compute a multidimensional integration over the likelihood and prior, which might be rather complicated. In this paper, we prefer to use the ICs instead of the Bayesian evidence to compare different dark energy models. This simpler approach is sufficient for our purpose.

Besides the ICs, we also apply the reduced χ^2 and the goodness-of-fit statistics to see how well the models fit the data. The reduced χ^2 is χ^2/ν, where ν denotes the degrees of freedom usually given by $N - k$. It describes how well a model fits the observational data sets. The goodness of fit (GoF) gives the probability of obtaining a larger discrepancy between the model and the data than that observed, assuming that the model is correct. It is defined as $\mathrm{GoF} = \Gamma(\nu/2, \chi^2/2)/\Gamma(\nu/2)$, where Γ is the incomplete gamma function.

3 CURRENT OBSERVATIONAL DATA SETS

In this section, we describe the latest data sets used in this paper and the method used to analyse them.

3.1 Type Ia supernovae

Currently, SNIa are the most powerful tool to study dark energy because of their role as standardizable candles. For the SNIa data, we use the current largest Union2.1 compilation (Suzuki et al. 2012), which contains a total of 580 SNIae. This is an updated version of the Union2 compilation (Amanullah et al. 2010). The 20 newly added SNe are all at a relatively high redshift ($0.6 < z < 1.4$), and thus they can help to tighten the constraints on the evolution behaviour of dark energy.

Cosmological constraints from SNIa data are obtained through the distance modulus $\mu(z)$. The theoretical distance modulus is

$$\mu_{\rm th}(z_i) = 5\log_{10} D_L(z_i) + \mu_0, \tag{3}$$

where $\mu_0 = 42.38 - 5\log_{10} h$, with h being the Hubble constant H_0 in units of 100 km s^{-1} Mpc^{-1}. The Hubble-free luminosity distance D_L is defined as

$$D_L(z) = \frac{1+z}{\sqrt{|\Omega_k|}}{\rm sinn}\left[\sqrt{|\Omega_k|}\int_0^z \frac{{\rm d}z'}{E(z')}\right], \tag{4}$$

where $E(z) = H(z)/H_0$ and Ω_k is the present curvature density. Here, the symbol sinn(x) stands for sinh(x) (if $\Omega_k > 0$), sin(x) (if $\Omega_k < 0$) or just x (if $\Omega_k = 0$).

To compute χ^2 for the SNIa data, we follow Nesseris & Perivolaropoulos (2005) to analytically marginalize over the nuisance parameter H_0:

$$\chi^2_{\rm SN} = A - 2\mu_0 B + \mu_0^2 C. \tag{5}$$

Here,

$$A = \sum_{i=1}^{580} \frac{[\mu_{\rm obs}(z_i) - \mu_{\rm th}(z_i;\mu_0 = 0)]^2}{\sigma_i^2},$$
$$B = \sum_{i=1}^{580} \frac{\mu_{\rm obs}(z_i) - \mu_{\rm th}(z_i;\mu_0 = 0)}{\sigma_i^2},$$
$$C = \sum_{i=1}^{580} \frac{1}{\sigma_i^2}, \tag{6}$$

where σ is the uncertainty in the SNIa data. Equation (5) has a minimum for $\mu_0 = B/C$ at

$$\tilde{\chi}^2_{\rm SN} = A - \frac{B^2}{C}. \tag{7}$$

This equation is independent of μ_0, so instead of $\chi^2_{\rm SN}$, we adopt $\tilde{\chi}^2_{\rm SN}$ to compute the likelihood.

3.2 Baryon acoustic oscillations

The competition between gravitational force and primordial relativistic plasma gives rise to acoustic oscillations, which leave their signature in every epoch of the Universe. As standard rulers, BAOs provide another independent test for constraining the property of dark energy.

Eisenstein et al. (2005) were the first to find a peak for these BAOs in the two-point correlation function at $100\,h^{-1}$ Mpc separation, measured from the Luminous Red Galaxy (LRG) sample of the SDSS Third Data Release (DR3), with effective redshift $z = 0.35$. Percival et al. (2010) have performed a power-spectrum analysis of the SDSS DR7 data set, considering both the main and LRG samples, and they have measured the BAO signal at both $z = 0.2$ and $z = 0.35$. Recently, in the low-redshift Universe, the 6dF Galaxy Survey (6dFGS) team has reported a BAO detection at $z = 0.1$ (Beutler et al. 2011). Most recently, Blake et al. (2011) have presented measurements of the BAO peak at redshifts $z = 0.44$, 0.6 and 0.73 in the galaxy correlation function of the final data set of the WiggleZ Dark Energy Survey. They have combined their WiggleZ BAO measurements with the SDSS DR7 and 6dFGS data sets to give tight constraints on dark energy. In this paper, we follow them, constraining different dark energy models using their combined BAO data set. We highlight our use of this combined BAO data set, because there are altogether six data points, which are more than previous BAO data, and few have used this combined BAO data set to constrain dark energy since the publication of the WiggleZ paper.

The data can be found in the above papers, but for completeness, here we summarize the BAO measurements and the way to use them.

The χ^2 for the WiggleZ BAO data is given by (Blake et al. 2011)

$$\chi^2_{\rm WiggleZ} = (\boldsymbol{A}_{\rm obs} - \boldsymbol{A}_{\rm th})C^{-1}_{\rm WiggleZ}(\boldsymbol{A}_{\rm obs} - \boldsymbol{A}_{\rm th})^{\rm T}, \tag{8}$$

where the data vector is $\boldsymbol{A}_{\rm obs} = (0.474, 0.442, 0.424)$ for the effective redshifts $z = 0.44$, 0.6 and 0.73, respectively. The corresponding theoretical value $\boldsymbol{A}_{\rm th}$ denotes the acoustic parameter $A(z)$ introduced by Eisenstein et al. (2005):

$$A(z) = \frac{D_V(z)\sqrt{\Omega_{\rm m}H_0^2}}{cz}. \tag{9}$$

The distance scale D_V is defined as

$$D_V(z) = \frac{1}{H_0}\left[(1+z)^2 D_{\rm A}(z)^2 \frac{cz}{E(z)}\right]^{1/3}, \tag{10}$$

where $D_{\rm A}(z)$ is the Hubble-free angular diameter distance, which relates to the Hubble-free luminosity distance through $D_{\rm A}(z) = D_L(z)/(1+z)^2$. The inverse covariance $C^{-1}_{\rm WiggleZ}$ is given by

$$C^{-1}_{\rm WiggleZ} = \begin{pmatrix} 1040.3 & -807.5 & 336.8 \\ -807.5 & 3720.3 & -1551.9 \\ 336.8 & -1551.9 & 2914.9 \end{pmatrix}. \tag{11}$$

Similarly, for the SDSS DR7 BAO distance measurements, the χ^2 can be expressed as (Percival et al. 2010)

$$\chi^2_{\rm SDSS} = (\boldsymbol{d}_{\rm obs} - \boldsymbol{d}_{\rm th})C^{-1}_{\rm SDSS}(\boldsymbol{d}_{\rm obs} - \boldsymbol{d}_{\rm th})^{\rm T}, \tag{12}$$

where $\boldsymbol{d}_{\rm obs} = (0.1905, 0.1097)$ are the data points at $z = 0.2$ and 0.35, respectively. Here, $\boldsymbol{d}_{\rm th}$ denotes the distance ratio

$$d_z = \frac{r_{\rm s}(z_{\rm d})}{D_V(z)}. \tag{13}$$

Here, $r_{\rm s}(z)$ is the comoving sound horizon,

$$r_{\rm s}(z) = c\int_z^\infty \frac{c_{\rm s}(z')}{H(z')}{\rm d}z', \tag{14}$$

where the sound speed $c_{\rm s}(z) = 1/\sqrt{3(1+\boldsymbol{R}_{\rm b}/(1+z))}$, with $\boldsymbol{R}_{\rm b} = 31\,500\Omega_{\rm b}h^2(T_{\rm CMB}/2.7\,{\rm K})^{-4}$ and $T_{\rm CMB} = 2.726$ K.

The redshift $z_{\rm d}$ at the baryon drag epoch is fitted with the formula proposed by Eisenstein & Hu (1998),

$$z_{\rm d} = \frac{1291(\Omega_{\rm m}h^2)^{0.251}}{1+0.659(\Omega_{\rm m}h^2)^{0.828}}\left[1 + b_1(\Omega_{\rm b}h^2)^{b_2}\right], \tag{15}$$

where

$$b_1 = 0.313(\Omega_{\rm m}h^2)^{-0.419}[1 + 0.607(\Omega_{\rm m}h^2)^{0.674}],$$
$$b_2 = 0.238(\Omega_{\rm m}h^2)^{0.223}. \tag{16}$$

In equation (12), $C^{-1}_{\rm SDSS}$ is the inverse covariance matrix for the SDSS data set given by

$$C^{-1}_{\rm SDSS} = \begin{pmatrix} 30\,124 & -17\,227 \\ -17\,227 & 86\,977 \end{pmatrix}. \tag{17}$$

For the 6dFGS BAO data (Beutler et al. 2011), there is only one data point at $z = 0.106$, and the χ^2 is easy to compute:

$$\chi^2_{\rm 6dFGS} = \left(\frac{d_z - 0.336}{0.015}\right)^2. \tag{18}$$

Thus, the total χ^2 for all the BAO data sets can be written as

$$\chi^2_{\rm BAO} = \chi^2_{\rm WiggleZ} + \chi^2_{\rm SDSS} + \chi^2_{\rm 6dFGS}. \tag{19}$$

3.3 Cosmic microwave background

Because the SNIa and BAO data contain information about the Universe at relatively low redshifts, we include the CMB information by using the *Wilkinson Microwave Anisotropy Probe* (*WMAP*) 7-yr data (Komatsu et al. 2011) to probe the entire expansion history up to the last scattering surface. The χ^2 for the CMB data is constructed as

$$\chi^2_{\rm CMB} = X^{\rm T} C^{-1}_{\rm CMB} X, \tag{20}$$

where

$$X = \begin{pmatrix} l_{\rm A} - 302.09 \\ R - 1.725 \\ z_* - 1091.3 \end{pmatrix}. \tag{21}$$

Here $l_{\rm A}$ is the 'acoustic scale', defined as

$$l_{\rm A} = \frac{\pi d_L(z_*)}{(1+z) r_{\rm s}(z_*)}. \tag{22}$$

Here, $d_L(z) = D_L(z)/H_0$, and the redshift of decoupling z_* is given by (Hu & Sugiyama 1996)

$$z_* = 1048 \left[1 + 0.00124(\Omega_{\rm b} h^2)^{-0.738}\right] \left[1 + g_1 (\Omega_{\rm m} h^2)^{g_2}\right], \tag{23}$$

$$g_1 = \frac{0.0783(\Omega_{\rm b} h^2)^{-0.238}}{1 + 39.5(\Omega_{\rm b} h^2)^{0.763}}, \quad g_2 = \frac{0.560}{1 + 21.1(\Omega_{\rm b} h^2)^{1.81}}, \tag{24}$$

The shift parameter R in equation (21) is defined as (Bond, Efstathiou & Tegmark 1997)

$$R = \frac{\sqrt{\Omega_{\rm m}}}{c(1+z_*)} D_L(z). \tag{25}$$

In equation (20), $C^{-1}_{\rm CMB}$ is the inverse covariance matrix:

$$C^{-1}_{\rm CMB} = \begin{pmatrix} 2.305 & 29.698 & -1.333 \\ 29.698 & 6825.270 & -113.180 \\ -1.333 & -113.180 & 3.414 \end{pmatrix}. \tag{26}$$

3.4 Observational Hubble data

In addition to the SNIa, BAO and CMB data, we also use the observational Hubble data (OHD) as an observational technique. These data compose an independent data set that can help break the parameter degeneracies, and thus it might also shed light on the cosmological models we aim to study.

In this paper, we adopt 11 data points from the differential ages of old passive evolving galaxies (Stern et al. 2010). The χ^2 value for these OHD can be expressed as

$$\chi^2_{\rm OHD} = \sum_{i=1}^{11} \frac{[H_{\rm th}(z_i) - H_{\rm obs}(z_i)]^2}{\sigma_i^2}, \tag{27}$$

where σ_i is the 1σ error in the OHD, with z_i ranging from 0.1 to 1.75.

4 COSMOLOGICAL MODELS AND CONSTRAINING RESULTS

In the following, we study eight popular cosmological models that have been discussed in the literature. Table 1 lists the models, with their parameters and the abbreviations we use. We examine them using the expansion history of the Universe to see whether they are consistent with current data at the background level. The model parameters are determined through the minimum χ^2 fitting by using the MCMC method. Our MCMC code is based on the publicly available COSMOMC package (Lewis & Bridle 2002).

Table 1. Summary of cosmological models. The Hubble constant H_0 in the fit is not deemed as a model parameter, but we include it in the number of degrees of freedom and in k when calculating the AIC and BIC.

Model	Abbreviation	Parameters
Cosmological constant	ΛCDM	Ω_k, $\Omega_{\rm m}$
Constant w	wCDM	Ω_k, $\Omega_{\rm m}$, w
Varying w (Chevalier–Polarski–Linder)	CPL	Ω_k, $\Omega_{\rm m}$, w_0, $w_{\rm a}$
Generalized Chaplygin gas	GCG	Ω_k, $A_{\rm s}$, α
Dvali–Gabadadze–Porrati	DGP	Ω_k, $\Omega_{\rm m}$
Modified polytropic Cardassian	MPC	Ω_k, $\Omega_{\rm m}$, q, n
Interacting dark energy	IDE	Ω_k, $\Omega_{\rm m}$, w_x, δ
Early dark energy	EDE	Ω_k, $\Omega_{\rm m}$, $\Omega_{\rm e}$, w_0

It should be stressed here that unlike most other work on dark energy model constraints, we do not assume a spatially flat universe as a prior in this paper, although recent studies have shown that the Universe is nearly flat (Komatsu et al. 2011). When we constrain the properties of dark energy, the parameters, such as the equation of state w, are always degenerate with the curvature density Ω_k. It has already been shown that ignoring Ω_k will induce large errors on the reconstructed dark energy parameter (e.g. w). If the true geometry is not flat and with the wrong flatness assumption, one will erroneously conclude the wrong behaviour of dark energy, even if the curvature term is very small (Clarkson, Cortês & Bassett 2007; Zhao et al. 2007; Virey et al. 2008). So, instead of assuming a flat universe, here we include Ω_k as a free parameter in different cosmological models.

4.1 Cosmological constant model

The cosmological constant Λ was originally introduced by Einstein (1917) to achieve a static universe, but it was later abandoned by Einstein after Hubble's discovery of the expansion of the Universe. Ironically, after 1998, the cosmological constant revived again as a form of dark energy responsible for the late-time acceleration of the Universe. The cosmological constant plus CDM is usually called the ΛCDM model, and in this model the dark energy equation of state $w = -1$ at all times. The Friedmann equation in this case is

$$\frac{H^2(z)}{H_0^2} = \Omega_k (1+z)^2 + \Omega_r (1+z)^4 + \Omega_{\rm m}(1+z)^3 + (1 - \Omega_k - \Omega_r - \Omega_{\rm m}), \tag{28}$$

where the radiation density parameter Ω_r is given by $\Omega_r = \Omega_\gamma(1 + 0.2271\, N_{\rm eff})$ with $\Omega_\gamma = 2.469 \times 10^{-5}\, h^{-2}$ and the effective number of neutrino species $N_{\rm eff} = 3.04$ (Komatsu et al. 2011). We caution that, in many papers, the Ω_r term is usually neglected. While this is reasonable for SNIa analyses where the redshift is very small, for high redshift, especially at the CMB epoch, this term is dominant. When calculating the sound horizon $r_{\rm s}$ for CMB and BAO analyses, ignoring this radiation term will induce large errors on the results, so it would be better to include it. The last term in the equation represents the energy density of the cosmological constant.

This simple model has only two parameters, Ω_k and $\Omega_{\rm m}$. Our global fitting from all the four data sets gives the best-fitting values with 1σ errors:

$$\Omega_k = -0.0024 \pm 0.0056, \qquad \Omega_{\rm m} = 0.291 \pm 0.014. \tag{29}$$

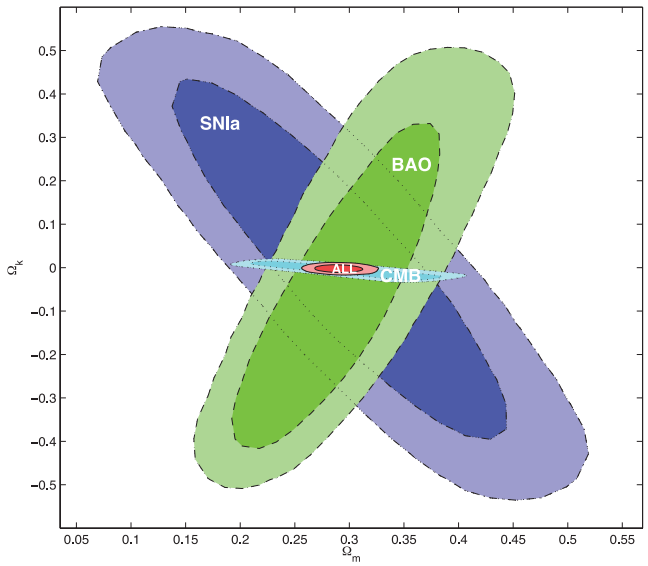

Figure 1. Marginalized 1σ and 2σ contours of the ΛCDM model parameters Ω_k and Ω_m, derived from different data sets. 'ALL' denotes the joint constraint including all four data sets.

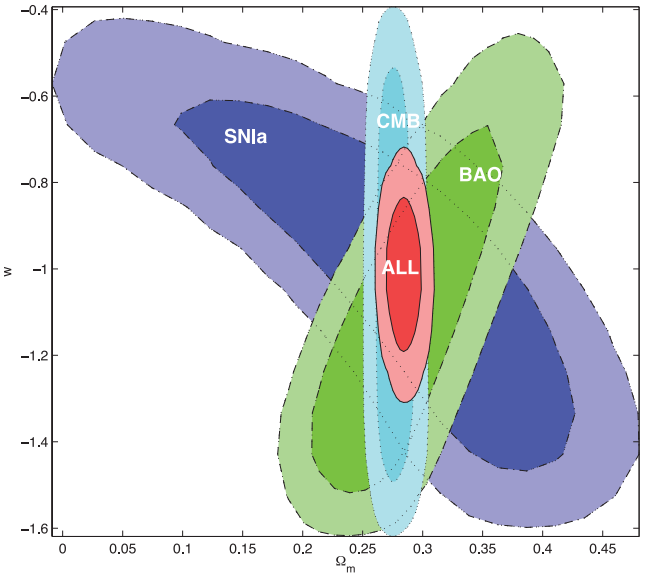

Figure 2. Marginalized 1σ and 2σ contours of the wCDM model parameters Ω_m and w, derived from different data sets. 'ALL' denotes the joint constraint including all four data sets.

Our results are consistent with the latest results of the WiggleZ BAO study (Blake et al. 2011). Fig. 1 shows the constraint from each of the SNIa, CMB and BAO data sets and the joint constraint from all four data sets. We do not give the constraint separately from OHD because currently it is not as stringent as the first three probes. However, we do include it in the combined results. It can be seen that although the contour of each single data set is quite broad, their combined constraint is quite stringent, and this reminds us of the power of joint analysis from different independent data sets. A flat universe is quite favoured by current data within 1σ confidence level.

4.2 Constant w model

The simplest extension to the ΛCDM model is to assume that the dark energy equation of state w does not precisely equal -1, but that it is a constant to be fitted with the data. In this model, the Friedmann equation is

$$\frac{H^2(z)}{H_0^2} = \Omega_k(1+z)^2 + \Omega_r(1+z)^4 + \Omega_m(1+z)^3 + (1-\Omega_k-\Omega_r-\Omega_m)(1+z)^{3(1+w)}. \quad (30)$$

There are three parameters in this model: Ω_k, Ω_m and w. The best-fitting values, using all the data sets, are

$$\Omega_k = -0.0012 \pm 0.0064, \qquad \Omega_m = 0.292 \pm 0.015, \qquad w = -0.990 \pm 0.041, \quad (31)$$

which also agree with Blake et al. (2011).

In Fig. 2, we plot the contours of Ω_m and w after marginalizing over Ω_k and H_0. This model also gives a good fit to different data sets. The combined result shows a clear preference around the cosmological constant model ($w = -1$ within the 1σ confidence level).

4.3 Chevallier–Polarski–Linder model

There is no prior reason to expect w to be -1 or a constant. If w varies with time, the Friedmann equation is modified as

$$\frac{H^2(z)}{H_0^2} = \Omega_k(1+z)^2 + \Omega_r(1+z)^4 + \Omega_m(1+z)^3 + (1-\Omega_k-\Omega_r-\Omega_m) \times \exp\left[3\int_0^z \frac{1+w(z')}{1+z'}\,\mathrm{d}z'\right]. \quad (32)$$

Many function forms of w evolving with redshift have been proposed so far (e.g. Johri & Rath 2007). Among the various parametrizations of the dark energy equation of state w, the one developed by Chevallier & Polarski (2001) and Linder (2003) turns out to be an excellent approximation to a wide variety of dark energy models. This Chevalier–Polarski–Linder (CPL) model is the most commonly used function form to study the time dependence of w. The equation of state in this model is

$$w(z) = w_0 + w_a\frac{z}{1+z}, \quad (33)$$

So, if we insert equation (33) into equation (32), we obtain the Friedmann equation for this CPL model:

$$\frac{H^2(z)}{H_0^2} = \Omega_k(1+z)^2 + \Omega_r(1+z)^4 + \Omega_m(1+z)^3 + (1-\Omega_k-\Omega_r-\Omega_m)\,(1+z)^{3(1+w_0+w_a)} \times \exp\left(\frac{-3w_a z}{1+z}\right). \quad (34)$$

There are four parameters in this model: Ω_k, Ω_m, w_0 and w_a. Our best-fitting values for these parameters are

$$\Omega_k = 0.00027^{+0.0034}_{-0.0051}, \qquad \Omega_m = 0.293 \pm 0.016, \qquad w_0 = -0.966^{+0.088}_{-0.105}, \qquad w_a = 0.202^{+1.030}_{-1.053}. \quad (35)$$

Fig. 3 shows the contours of w_0 and w_a for the CPL model after they are marginalized over other parameters. Obviously, w_a is weakly constrained by the current data. This is partially because of

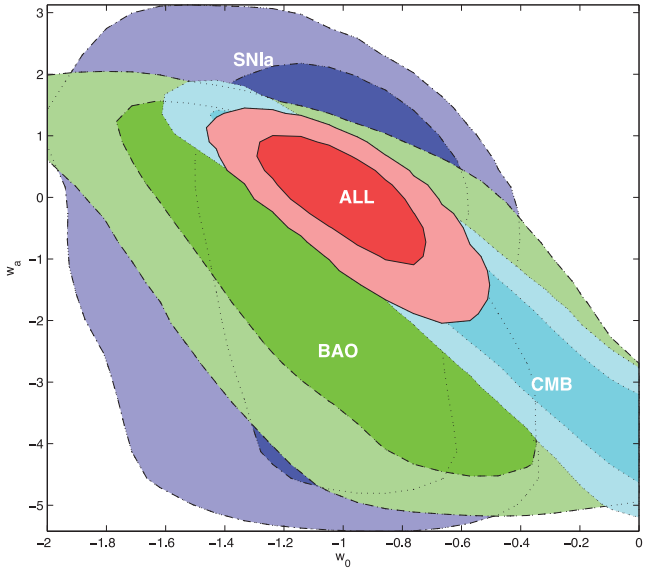

Figure 3. Marginalized 1σ and 2σ contours of the CPL model parameters w_0 and w_a, derived from different data sets. 'ALL' denotes the joint constraint including all four data sets.

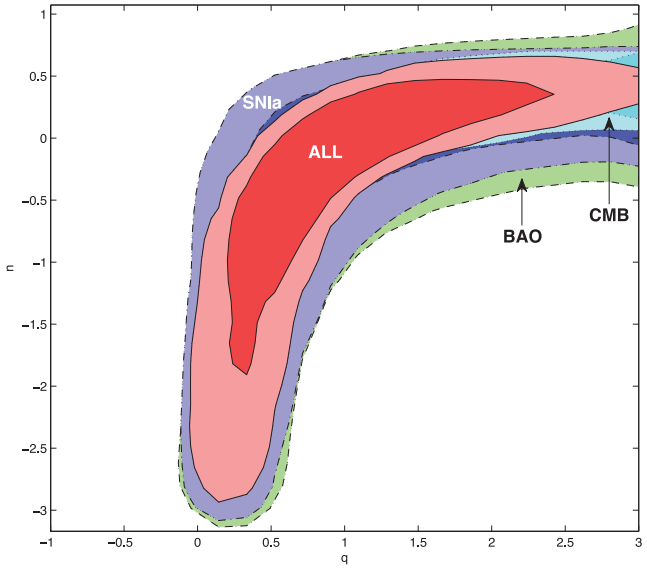

Figure 4. Marginalized 1σ and 2σ contours of the MPC model parameters q and n, derived from different data sets. 'ALL' denotes the joint constraint including all four data sets.

the degeneracy between the curvature and the equation of state. If we were to set $\Omega_k = 0$ in the fit, as most authors do, the constraints would be more stringent, especially for a single data set. However, as explained earlier, we do not assume a flat prior in the fitting procedure. We see once again that it is consistent with the ΛCDM model for $w_0 = -1$ and $w_a = 0$. Our results are in agreement with the results of Blake et al. (2011), although they have assumed a flat universe in their fit.

4.4 Modified polytropic Cardassian expansion

The Cardassian expansion model was first proposed by Freese & Lewis (2002). It modifies the Friedmann equation to allow for acceleration in a matter-dominated universe. The motivation for this modification could be the embedding of our observable Universe living as a three-dimensional brane in a higher-dimensional universe. The original form of the Cardassian model can be written as

$$H^2(z) = \frac{8\pi G}{3}\rho_{\rm m} + B\rho_{\rm m}^n, \tag{36}$$

where B is a constant and n is a dimensionless parameter.

This power-law form is equivalent to the constant w model (Section 4.2) for $w = n - 1$, so there is no need to additionally fit this model. Here, we consider a modified polytropic Cardassian (MPC) model proposed by Wang et al. (2003). In addition, we also include the curvature and radiation term:

$$\frac{H^2(z)}{H_0^2} = \Omega_k(1+z)^2 + \Omega_r(1+z)^4 + \Omega_{\rm m}(1+z)^3 \times \left\{1 + \left[\left(\frac{1-\Omega_k-\Omega_r}{\Omega_{\rm m}}\right)^q - 1\right](1+z)^{3q(n-1)}\right\}^{1/q}. \tag{37}$$

The above equation reduces to the ΛCDM equation for $q = 1$ and $n = 0$. Our joint constraints give the best-fitting parameters as follows:

$$\Omega_k = 0.0022 \pm 0.0025, \qquad \Omega_{\rm m} = 0.280 \pm 0.006,$$
$$q = 0.897^{+0.152}_{-0.468}, \qquad n = -0.648^{+0.856}_{-1.106}. \tag{38}$$

The constraints on the parameter q and n is very weak from the current data. Fig. 4 displays the marginalized contours of q and n. It can be seen that it is still consistent with the ΛCDM model at the 1σ level.

4.5 Dvali–Gabadadze–Porrati model

The Dvali–Gabadadze–Porrati (DGP) model is a popular model, which modifies the gravity to allow for cosmic acceleration without dark energy (Dvali, Gabadadze & Porrati 2000). This model might arise from the brane world theory, in which gravity leaks out into the bulk at large scales. The Friedmann equation is modified as

$$\frac{H^2(z)}{H_0^2} = \Omega_k(1+z)^2 + \Omega_r(1+z)^4 + \left[\sqrt{\Omega_{\rm m}(1+z)^3 + \Omega_{r_{\rm c}}} + \sqrt{\Omega_{r_{\rm c}}}\right]^2, \tag{39}$$

where $r_{\rm c}$ is the length-scale beyond which gravity leaks out into the bulk and $\Omega_{r_{\rm c}} = 1/(4r_{\rm c}^2H_0^2)$. Setting $z = 0$ in equation (39), we obtain the normalization condition:

$$\Omega_{r_{\rm c}} = \frac{(1-\Omega_{\rm m}-\Omega_r-\Omega_k)^2}{4(1-\Omega_k-\Omega_r)}. \tag{40}$$

The DGP model has the same number of parameters as the ΛCDM model. The marginalized best-fitting parameters are

$$\Omega_k = 0.020 \pm 0.006, \qquad \Omega_{\rm m} = 0.305 \pm 0.015. \tag{41}$$

We can see that although the matter density is consistent with that of the ΛCDM model, the curvature term is much larger than that in other models. This feature has also been noticed by Zhu & Alcaniz (2005) and Guo et al. (2006), who obtained a non-flat universe for the DGP model at a high confidence level. In Fig. 5, it can be seen that the three observational probes strongly disagree – the areas of intersection of any pair are distinct from other pairs. The CMB data prefer a positive Ω_k while SN and BAO data are in support of negative Ω_k. Rubin et al. (2009) and Davis et al. (2007) have also noticed this signal. It could imply that this DGP model is strongly

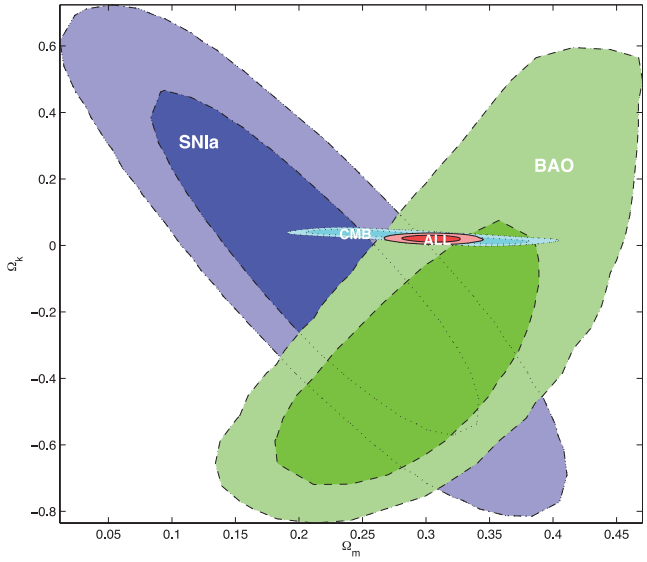

Figure 5. Marginalized 1σ and 2σ contours of the DGP model parameters Ω_m and Ω_k, derived from different data sets. 'ALL' denotes the joint constraint including all four data sets.

disfavoured by the current data. This can be further quantified by the model selection statistics, which are shown in Section 5.

It should be mentioned that the DGP model could perform better when using only SNIa data. For example, using the MLCS2k2 light-curve fitter for SDSS-II SN data, Sollerman et al. (2009) have found that the DGP model performs better than the ΛCDM model under the ICs. Also, recently, it has been noticed that the SNLS3 data, analysed with SALT2 fitters alone, prefer the DGP model over others (Li, Wu & Yu 2012). However, when combined with BAO and CMB data, things changed, and the concordance ΛCDM model became favoured. This is not surprising, because the current SNIa data are mainly confined by systematic errors rather than statistical errors, so it would be better to combine the SNIa data set with other probes (BAO, CMB, etc.) to constrain cosmological models. This would avoid any potential bias that might be caused by the systematics of SNIa.

4.6 Interacting dark energy model

The fact that the energy density of dark energy is the same order as that of dark matter in the present Universe suggests that there might be some relations between them. This could arise from the interaction between a scalar field (e.g. quintessence field) and dark matter. Such a motivation might help to alleviate the coincidence problem. A popular approach to study this interaction is to introduce a coupling term on the right-hand side of the continuity equations (Dalal et al. 2001; Cai & Wang 2005; Guo, Ohta & Tsujikawa 2007; Caldera-Cabral, Maartens & Ureña-López 2009):

$$\dot{\rho}_m + 3H\rho_m = +\Gamma\rho_m,$$

$$\dot{\rho}_x + 3H(1+w_x)\rho_x = -\Gamma\rho_m, \tag{42}$$

where Γ characterizes the strength of the interaction, ρ_m is the matter density, ρ_x is the dark energy density and w_x is the equation of state of dark energy. In order to place observational constraints on the coupling term Γ, it is convenient to express Γ in terms of the Hubble parameter H

$$\Gamma = \delta H, \tag{43}$$

where δ is a dimensionless coupling term. Note that a positive δ corresponds to a transfer of energy from dark energy to dark matter, whereas for a negative δ the energy transfer is the opposite.

It is obvious that the expansion history will depend on the parameter δ, and thus we are interested in placing observational constraints on it. For simplicity, here we assume that δ is a constant. In the more general case, δ might be varying, and there has already been a lot of work carried out on this varying case. In this paper, because we mainly focus on the model comparison, the study of a constant coupling is enough for our purpose.

For a constant δ, solving equation (42) with equation (43), the Friedmann equation becomes

$$\frac{H^2(z)}{H_0^2} = \Omega_k(1+z)^2 + \Omega_r(1+z)^4 + (1-\Omega_m-\Omega_k-\Omega_r) \times (1+z)^{3(1+w_x)} + \frac{\Omega_m}{\delta+3w_x} \times \left[\delta(1+z)^{3(1+w_x)} + 3w_x(1+z)^{3-\delta}\right]. \tag{44}$$

This model has four parameters: Ω_k, Ω_m, w_x and δ. The concordance ΛCDM model is recovered for $\delta = 0$ and $w_x = -1$. Our global fitting gives the following best-fitting values:

$$\Omega_k = 0.0007 \pm 0.0032, \quad \Omega_m = 0.292 \pm 0.007, \quad \delta = -0.0043 \pm 0.0066, \quad w_x = -1.001 \pm 0.087. \tag{45}$$

Fig. 6 shows the case for this interacting dark energy (IDE) model. It is noticed that the SNIa and BAO data sets give quite weak constraints on the parameter space, comparing to the CMB data set. This is not strange because the SNIa and BAO data are located in low redshifts, and we can see from equation (44) that when $z \ll 1$ the $\delta + 3w_x$ term just cancels out, so the corresponding information about δ is lost. This tells us how important it is to include other high-redshift data. The CMB data and OHD are appropriate for this purpose. Our results show that the ΛCDM model still remains a good fit to the data (at least within the 2σ level), but a negative coupling ($\delta < 0$; i.e. the energy transfers from dark matter to dark energy) is slightly favoured. Also, in this case, the equation of state of dark energy w_x prefers a phantom case $w_x < -1$. This result

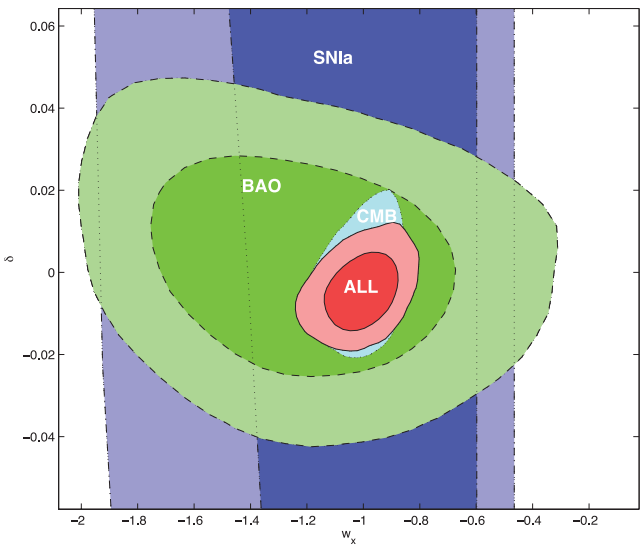

Figure 6. Marginalized 1σ and 2σ contours of the IDE model parameters δ and w_x, derived from different data sets. 'ALL' denotes the joint constraint including all four data sets.

is consistent with that obtained by other authors (Guo et al. 2007; Väliviita, Maartens & Majerotto 2010; Cao, Liang & Zhu 2011).

4.7 Generalized Chaplygin gas model

Despite their quite different properties in the equation of state and clustering, from the beginning, many researchers have been tempted to unify dark energy and dark matter in a single entity. To realize this, a natural and simple way is to introduce a perfect background fluid. The Chaplygin gas model is a typical example.

The original Chaplygin gas model was proposed by Kamenshchik, Moschella & Pasquier (2001). In this model, the pressure P of the fluid is related to its energy density ρ through $P = -A/\rho$, where A is a positive constant. In a more general case, it is possible to consider a generalized Chaplygin gas (GCG) model given by (Bento, Bertolami & Sen 2002)

$$P = -A\rho^{\alpha}. \tag{46}$$

Considering the energy conservation in the framework of the Friedmann–Robertson–Walker (FRW) metric, we obtain the following solution

$$\rho(a) = \rho_0 \left[A_{\rm s} + \frac{1 - A_{\rm s}}{a^{3(1+\alpha)}} \right]^{1/(1+\alpha)}, \tag{47}$$

where $A_{\rm s} = A/\rho_0^{1+\alpha}$ and ρ_0 is the present energy density of the GCG model. We find the intriguing feature that the energy density of this GCG model acts like dust matter at the early time and behaves as a cosmological constant at a late epoch. So, the GCG model can account for both dark matter and dark energy at the background level. The Friedmann equation for this model can be written as

$$\begin{aligned} \frac{H^2(z)}{H_0^2} &= \Omega_k(1+z)^2 + \Omega_r(1+z)^4 + \Omega_{\rm b}(1+z)^3 \\ &\quad + (1 - \Omega_k - \Omega_r - \Omega_{\rm b}) \\ &\quad \times \left[A_{\rm s} + (1 - A_{\rm s})(1+z)^{3(1+\alpha)} \right]^{1/(1+\alpha)}, \end{aligned} \tag{48}$$

where $\Omega_{\rm b}$ is the present density parameter of baryonic matter. We adopt $\Omega_{\rm b} = 0.0451$, according to the *WMAP* 7-yr results (Komatsu et al. 2011). The effective total matter density can be expressed as $\Omega_{\rm m} = \Omega_{\rm b} + (1 - \Omega_{\rm b} - \Omega_k - \Omega_r)(1 - A_{\rm s})^{1/(1+\alpha)}$. Note that the concordance ΛCDM model is recovered by $\alpha = 0$, and thus $\Omega_{\rm m} = 1 - \Omega_k - \Omega_r - A_{\rm s}(1 - \Omega_{\rm b} - \Omega_k - \Omega_r)$.

There are three parameters in this model. The fitting results are

$$\Omega_k = 0.0004 \pm 0.0032, \qquad A_{\rm s} = 0.733 \pm 0.025,$$

$$\alpha = -0.011 \pm 0.140. \tag{49}$$

The GCG model provides a good fit to the data. Fig. 7 shows the contours for the two parameters $A_{\rm s}$ and α in this GCG model. It can be seen that the ΛCDM model ($\alpha = 0$) falls well within the 1σ level, and the original Chaplygin gas model ($\alpha = 1$) is ruled out at more than the 2σ confidence level. This is in agreement with the results of Liang, Xu & Zhu (2011) and Wu & Yu (2007).

4.8 Early dark energy scenario

One of the differences between dynamical dark energy and the cosmological constant is that the energy density of the former might be non-negligible even at very high redshift (e.g. around recombination, or earlier). The existence of the so-called 'tracker' field (Steinhardt, Wang & Zlatev 1999) is important in order to alleviate

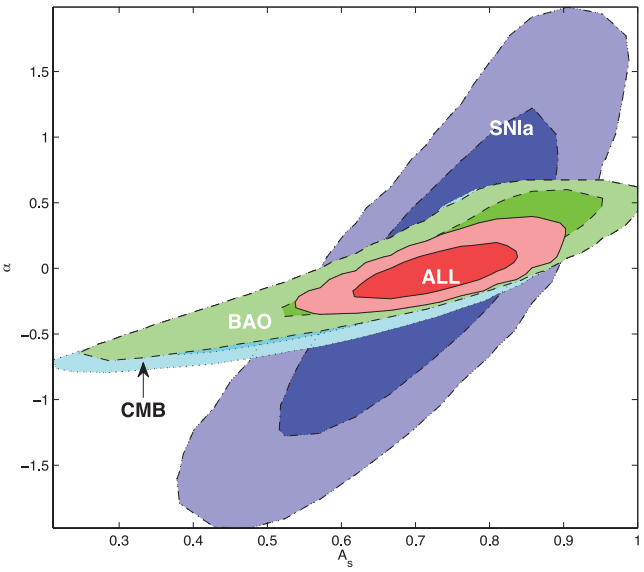

Figure 7. Marginalized 1σ and 2σ contours of the GCG model parameters $A_{\rm s}$ and α, derived from different data sets. 'ALL' denotes the joint constraint including all four data sets.

the cosmological constant problem. The tracker fields correspond to attractor-like solutions in which the field energy density tracks the background fluid density for a wide range of initial conditions. These models can be motivated by dilatation symmetry in particle physics and string theory (Wetterich 1988).

As a specific model of such an early dark energy (EDE) scenario, here we consider a commonly used form, with the dark energy density expressed as (Doran & Robbers 2006)

$$\Omega_{\rm DE}(z) = \frac{\Omega_{\rm DE}^0 - \Omega_{\rm e}\left[1 - (1+z)^{3w_0}\right]}{\Omega_{\rm DE}^0 + \Omega_{\rm m}(1+z)^{-3w_0}} + \Omega_{\rm e}\left[1 - (1+z)^{3w_0}\right], \tag{50}$$

where $\Omega_{\rm DE}^0$ is the present dark energy density, $\Omega_{\rm e}$ is the asymptotic EDE density and w_0 is the present dark energy equation of state. This equation is based on simple considerations, as depicted in Doran & Robbers (2006) and Doran, Schwindt & Wetterich (2001). The EDE behaviour is included in the $\Omega_{\rm e}$ term. The $-3w_0$ term, motivated by the relation $\Omega_{\rm DE}(z)/\Omega_{\rm m}(z) \propto (1+z)^{3w}$, allows the deviation from the ΛCDM model.

Equation (50) assumes a spatially flat universe. In this paper, because we do not assume flatness from the beginning, we would like to slightly modify equation (50) to include a contribution from curvature:

$$\begin{aligned} \Omega_{\rm DE}(z) &= \left\{\Omega_{\rm DE}^0 - \Omega_{\rm e}\left[1 - (1+z)^{3w_0}\right]\right\}\left[\Omega_{\rm DE}^0 + \Omega_{\rm m}\right. \\ &\quad \times (1+z)^{-3w_0} + \Omega_r(1+z)^{-3w_0+1} \\ &\quad \left. + \Omega_k(1+z)^{-3w_0-1}\right]^{-1} + \Omega_{\rm e}\left[1 - (1+z)^{3w_0}\right]. \end{aligned} \tag{51}$$

Here, $\Omega_{\rm DE}^0 = 1 - \Omega_{\rm m} - \Omega_r - \Omega_k$.

In this case, the Friedmann equation can be expressed as

$$\frac{H^2(z)}{H_0^2} = \frac{\Omega_{\rm m}(1+z)^3 + \Omega_r(1+z)^4 + \Omega_k(1+z)^2}{1 - \Omega_{\rm DE}(z)}. \tag{52}$$

This model also has four parameters. The best-fitting values are

$$\begin{aligned} &\Omega_k = 0.0042 \pm 0.0069, \qquad \Omega_{\rm m} = 0.291 \pm 0.007, \\ &\Omega_{\rm e} = 0.026^{+0.007}_{-0.026}, \qquad w_0 = -1.039 \pm 0.097. \end{aligned} \tag{53}$$

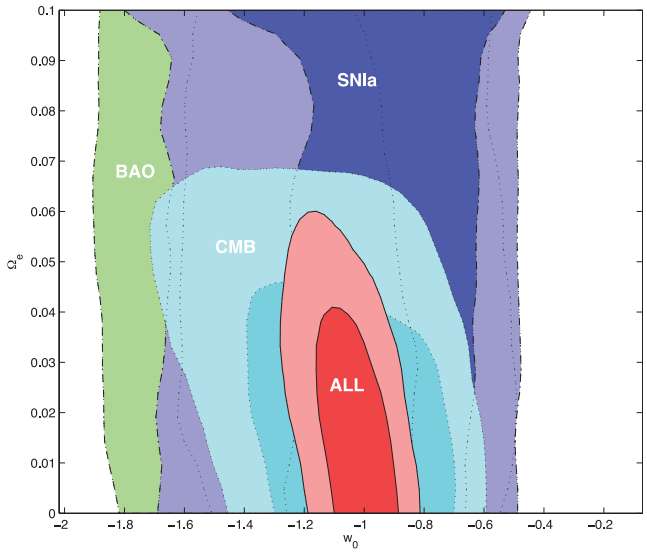

Figure 8. Marginalized 1σ and 2σ contours of the EDE model parameters w_0 and Ω_e, derived from different data sets. 'ALL' denotes the joint constraint including all four data sets.

As we can see from Fig. 8, the ΛCDM model ($\Omega_e = 0$, $w_0 = -1$) is still favoured within the 2σ level. However, the EDE component is not totally excluded from the current data. Because the SNIa and BAO data sets are low-redshift data sets, they cannot give effective constraints on the EDE density Ω_e. Thus, the most stringent constraint comes from the CMB data set. The results are consistent with those of Rubin et al. (2009), Calabrese et al. (2011) and Reichardt et al. (2012).

5 COMPARISON OF MODELS

In this section, we compare the different models by using the model selection statistics. Table 2 gives a summary of the IC results. It is easy to see that the concordance ΛCDM model has the lowest ICs, so the ΔAIC and ΔBIC are all calculated with respect to the ΛCDM model.

Given the current data sets, the ΛCDM model is clearly preferred by these model selection tests. Following this, there is a series of models that give comparably good fits but have more parameters. According to their ICs, we can roughly rank these models into four groups: group 1, positive against (GCG, wCDM); group 2, strong against (IDE, EDE); group 3, very strong against (MPC, CPL); group 4, essentially no support (DGP) from the current data. The GCG and wCDM models fit the data well, perhaps because they have fewer parameters and they can easily reduce to the ΛCDM model. The IDE and EDE models are punished by the ICs mainly because they have more parameters. The constraints on the MPC and CPL models are very weak, and they are also penalized by their large number of parameters. We see that the DGP model is strongly disfavoured by the data because its ΔICs have much larger values than others. Its GoF is also much smaller than the others. So we can say, at least at the background level, that the DGP model can be excluded by current joint data sets at high significance from a model selection point of view.

Table 2. Summary of the IC results. The ΛCDM model is preferred by both the AIC and the BIC. Thus, the ΔAIC and ΔBIC values for all other models are measured with respect to the ΛCDM model. The models are listed in order of increasing ΔAIC. The GoF approximates the probability of finding a worse fit to the data.

Model	χ^2/dof	GoF (per cent)	ΔAIC	ΔBIC
ΛCDM	555.98/597	88.42	0.00	0.00
GCG	555.64/596	88.04	1.66	6.06
wCDM	555.96/596	87.85	1.98	6.38
IDE	555.02/595	87.83	3.04	11.83
EDE	555.06/595	87.81	3.08	11.87
MPC	555.56/595	87.50	3.58	12.37
CPL	555.94/595	87.26	3.96	12.75
DGP	567.98/597	76.79	13.01	13.01

To see more clearly how to realize cosmic acceleration from these models, we plot the deceleration parameter q in Fig. 9. The deceleration parameter q, defined as $q = -\ddot{a}a/\dot{a}^2$, can be calculated by

$$q = -1 + \frac{1+z}{H(z)}\frac{\mathrm{d}H(z)}{\mathrm{d}z}. \tag{54}$$

As expected, these models all give negative q at late times, and positive q at an earlier epoch, meaning that the expansion of the Universe slowed down in the past and speeded up recently. Phenomenologically, there is a transition redshift z_t between the two epochs, and we also show this in the figure. We can see from Fig. 9 that because of their complexity, the constraints on the CPL and MPC models are very weak, as are the contours of their parameters. Although the constraint on the DGP model is quite tight, it gives the transition redshift $z_t = 0.45$, which is much smaller than the other models, suggesting a strong distinction between the DGP model and the other models. Given the bad behaviour of the DGP model from the model selection techniques discussed earlier, this smaller transition redshift might also suggest that the DGP model is disfavoured by the current data. The concordance ΛCDM model remains the best fit in the figure.

6 DISCUSSION AND CONCLUSION

We have studied a number of different cosmological models in the light of the latest observational data. The data we have used include the newly published Union2.1 SNe compilation and the WiggleZ BAO measurements, together with the *WMAP* 7-yr distance priors and the observational Hubble data. By using these data sets, we have obtained the best-fitting parameters for different models. We use the ICs, including the AIC and the BIC, to compare different models and to see which is the model most favoured by the current data. These ICs tend to favour models that give a good fit with fewer parameters. Unlike many authors previously, we do not assume a spatially flat universe; instead, we treat the spatial curvature Ω_k as a free parameter in the fitting procedure.

Using the AIC and BIC to compare models, we find that the concordance ΛCDM model remains the best model to explain the current data. The GCG model and the constant w model also give good fits to the data. The IDE model, the EDE scenario, the CPL model and the MPC model are all penalized by their large numbers of parameters, and thus they are not favoured by the ICs. The DGP model gives the worst fit, although it has the same number of parameters as the ΛCDM model. Its AIC and BIC are much larger than other models, with a bad GoFt. Meanwhile, the curvature density parameter Ω_k is quite near zero for all models except for the DGP model. In the DGP model, the different contours from the different observational data sets strongly disagree – SNIa and BAO prefer negative values of Ω_k whereas the CMB prefers positive Ω_k – and

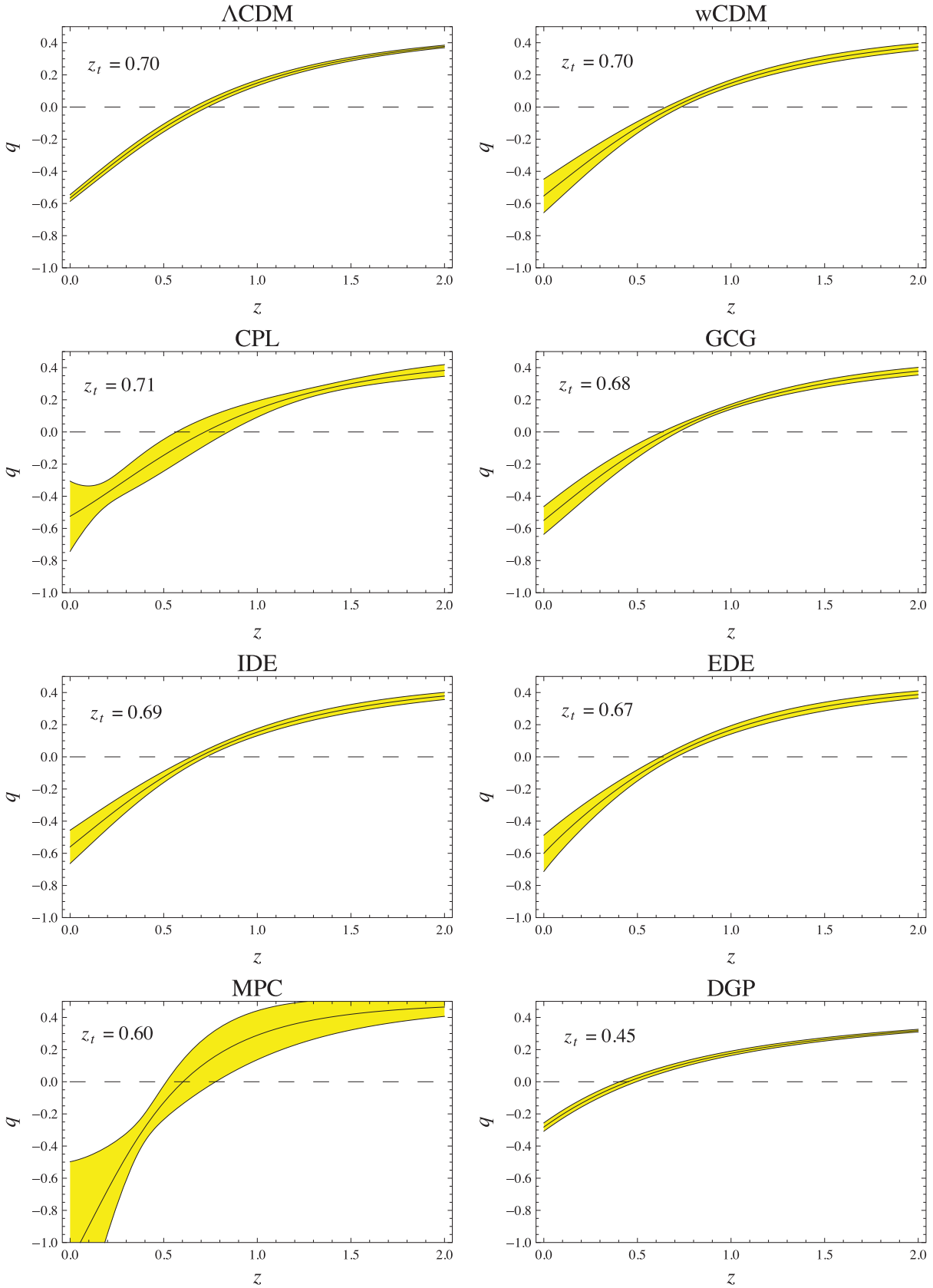

Figure 9. Evolution of the deceleration parameter q for different cosmological models (the shaded regions show the 1σ uncertainties). The corresponding transition redshift z_t is also given in each panel.

so the joint constraint on the value of Ω_k is much larger than in other models.

We have also shown the deceleration parameter q for different models, and we find that all models indicate a late-time cosmic acceleration, consistent with observations. However, the transition redshift z_t for the DGP model is much smaller than that in other models. This might reflect the fact that the DGP model cannot reduce to the concordance ΛCDM model for any value of its parameters.

In brief, given the current data sets, the ΛCDM model remains the best model from a model-comparison point of view, followed by those that can reduce to it. Those models that cannot reduce to the concordance model fit the data quite badly, especially the DGP model. In spite of its observational success, because of theoretical considerations, we cannot yet say that this ΛCDM model truly describes our Universe. For the time being, we can, at most, conclude that this model best fits the current data among various models. As more and more precise data become available in the future, it is excepted that we will finally be able to identify the nature of cosmic acceleration.

ACKNOWLEDGMENTS

KS thanks Shi Qi for helpful comments and discussions. The authors are also grateful to the anonymous referee for helpful comments and suggestions. This work was supported by the National Natural Science Foundation of China (grant nos. 10973039 and 11033002) and the National Basic Research Programme of China (973 programme, grant no. 2009CB824800).

REFERENCES

Akaike H., 1974, IEEE Trans. Automatic Control, 19, 716
Amanullah R. et al., 2010, ApJ, 716, 712
Bento M. C., Bertolami O., Sen A. A., 2002, Phys. Rev. D, 66, 043507
Beutler F. et al., 2011, MNRAS, 416, 3017
Blake C. et al., 2011, MNRAS, 1598
Bond J. R., Efstathiou G., Tegmark M., 1997, MNRAS, 291, L33
Burnham K. P., Anderson D. R., 2003, Technometrics, 45, 181
Cai R.-G., Wang A., 2005, J. Cosmol. Astropart. Phys., 3, 2
Calabrese E., Huterer D., Linder E. V., Melchiorri A., Pagano L., 2011, Phys. Rev. D, 83, 123504
Caldera-Cabral G., Maartens R., Ureña-López L. A., 2009, Phys. Rev. D, 79, 063518
Cao S., Liang N., Zhu Z.-H., 2011, MNRAS, 416, 1099
Chevallier M., Polarski D., 2001, Int. J. Mod. Phys. D, 10, 213
Clarkson C., Cortês M., Bassett B., 2007, J. Cosmol. Astropart. Phys., 8, 11
Copeland E. J., Sami M., Tsujikawa S., 2006, Int. J. Mod. Phys. D, 15, 1753
Dalal N., Abazajian K., Jenkins E., Manohar A. V., 2001, Phys. Rev. Lett., 87, 141302
Davis T. M. et al., 2007, ApJ, 666, 716
Doran M., Robbers G., 2006, J. Cosmol. Astropart. Phys., 6, 26
Doran M., Schwindt J.-M., Wetterich C., 2001, Phys. Rev. D, 64, 123520
Dvali G., Gabadadze G., Porrati M., 2000, Phys. Lett. B, 485, 208
Einstein A., 1917, Sitzungsber. Preuss. Akad. Wiss. Berlin (Math. Phys.), 142, 235
Eisenstein D. J., Hu W., 1998, ApJ, 496, 605
Eisenstein D. J. et al., 2005, ApJ, 633, 560
Freese K., Lewis M., 2002, Phys. Lett. B, 540, 1
Frieman J. A., Turner M. S., Huterer D., 2008, ARA&A, 46, 385
Guo Z.-K., Zhu Z.-H., Alcaniz J. S., Zhang Y.-Z., 2006, ApJ, 646, 1
Guo Z.-K., Ohta N., Tsujikawa S., 2007, Phys. Rev. D, 76, 023508
Hu W., Sugiyama N., 1996, ApJ, 471, 542
Johri V. B., Rath P. K., 2007, Int. J. Mod. Phys. D, 16, 1581
Kamenshchik A., Moschella U., Pasquier V., 2001, Phys. Lett. B, 511, 265
Komatsu E. et al., 2011, ApJS, 192, 18
Lewis A., Bridle S., 2002, Phys. Rev. D, 66, 103511
Li Z., Wu P., Yu H., 2012, ApJ, 744, 176
Liang N., Xu L., Zhu Z.-H., 2011, A&A, 527, A11
Liddle A. R., 2004, MNRAS, 351, L49
Liddle A. R., 2007, MNRAS, 377, L74
Linder E. V., 2003, Phys. Rev. Lett., 90, 091301
Nesseris S., Perivolaropoulos L., 2005, Phys. Rev. D, 72, 123519
Percival W. J. et al., 2010, MNRAS, 401, 2148
Perlmutter S. et al., 1999, ApJ, 517, 565
Reichardt C. L., de Putter R., Zahn O., Hou Z., 2012, ApJ, 749, L9
Riess A. G. et al., 1998, AJ, 116, 1009
Robert E. K., Adrian E. R., 1995, J. Am. Stat. Assoc., 90, 773
Rubin D. et al., 2009, ApJ, 695, 391
Saini T. D., Weller J., Bridle S. L., 2004, MNRAS, 348, 603
Schwarz G., 1978, Ann. Stat., 6, 461
Sollerman J. et al., 2009, ApJ, 703, 1374
Spergel D. N. et al., 2003, ApJS, 148, 175
Steinhardt P. J., Wang L., Zlatev I., 1999, Phys. Rev. D, 59, 123504
Stern D., Jimenez R., Verde L., Kamionkowski M., Stanford S. A., 2010, J. Cosmol. Astropart. Phys., 2, 8
Sullivan M. et al., 2011, ApJ, 737, 102
Suzuki N. et al., 2012, ApJ, 746, 85
Trotta R., 2007, MNRAS, 378, 72
Väliviita J., Maartens R., Majerotto E., 2010, MNRAS, 402, 2355
Virey J.-M., Talon-Esmieu D., Ealet A., Taxil P., Tilquin A., 2008, J. Cosmol. Astropart. Phys., 12, 8
Wang Y., Freese K., Gondolo P., Lewis M., 2003, ApJ, 594, 25
Weinberg S., 1989, Rev. Mod. Phys., 61, 1
Wetterich C., 1988, Nucl. Phys. B, 302, 668
Wu P., Yu H., 2007, ApJ, 658, 663
Zhao G.-B., Xia J.-Q., Li H., Tao C., Virey J.-M., Zhu Z.-H., Zhang X., 2007, Phys. Lett. B, 648, 8
Zhu Z.-H., Alcaniz J. S., 2005, ApJ, 620, 7

This paper has been typeset from a TEX/LATEX file prepared by the author.